

Introduction: Seismicity estimates play an important role in creating regional geological characterizations, which are useful for understanding a planet’s formation and evolution, and of key importance to site selection for landed missions. Here we investigate the regional effects of lunar seismicity with the goal of determining whether surface features such as landslides and boulder trails on the Moon are triggered by fault motion (Fig. 1).

Lobate scarps: Lobate scarps, the typical surface expressions of thrust faults resulting from tectonic compression, are widely observed on the Moon [1]. Compared to other types of tectonic faults, surface-cutting thrust faults require the largest amount of stress to form and/or slip, and thus are expected to result in large quakes. While normal faults, graben, and wrinkle ridges are also abundant on the Moon, these structures would generate smaller theoretical maximum quakes than lobate scarp thrust faults. Thus, we optimize our chances of finding mass wasting associated with faults by studying lobate scarps.

Methodology: We first calculate the theoretical maximum quake that could occur as a result of slip on a fault and then determine the effects on the surrounding surface morphology. The expected damage area indicated by seismic wavefield modeling is compared to mapped imagery to determine the likelihood of a quake having triggered mass wasting.

Theoretical maximum quake. Following the method outlined in [2], the theoretical maximum quake magnitude is derived from basic fault properties. These are either estimated from imagery or derived from laboratory rock experiments or elastic dislocation models, and include the fault length, width, dip angle, and depth of faulting. Fault displacement is calculated using displacement-length scaling such that $D=\gamma L$, where γ is determined by rock type and tectonic setting [3].

The best measure of the size of a quake is the seismic moment, which is calculated by multiplying the shear modulus of the ruptured rock by the area of the ruptured portion of the fault and the average displacement produced during the quake [2]. The seismic moment represents the total energy consumed in producing displacement on a fault, regardless of the local strain rate or fault formation mechanism.

Seismic wavefield modeling. In order to determine the dimensions of an area affected by seismic shaking, we model the ground motion resulting from the theoretical maximum quake along a given fault. We use the

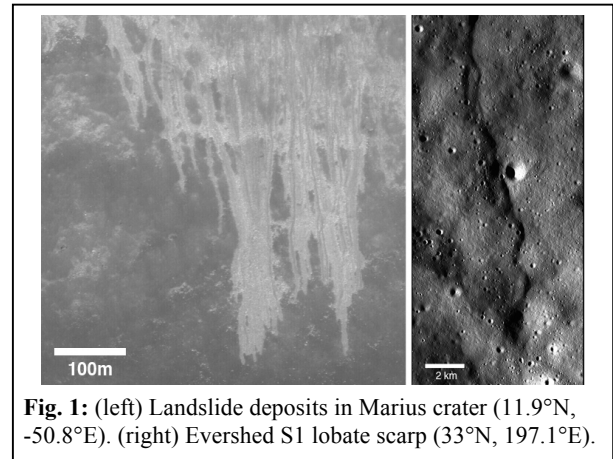


Fig. 1: (left) Landslide deposits in Marius crater (11.9°N, -50.8°E). (right) Evershed S1 lobate scarp (33°N, 197.1°E).

Serpentine Wave Propagation Program (WPP), a numerical code for simulating seismic wave propagation in 3D [4, 5]. The initial model of a given fault includes regional topography derived from digital elevation models, and the Moon’s background 1D velocity.

Geomorphological analysis: Peak vertical ground motion occurs within a few kilometers of the main shock and drops off rapidly away from the source. Thus we should expect most of the mass wasting phenomena to occur in the immediate vicinity of the fault. However, this result may depend on regional effects such as surface slope and megaregolith thickness; a thicker megaregolith (as might be expected in the vicinity of large craters) would tend to focus shaking in some of the crater basins.

We will compare the observed extent of mass wasting in the vicinity of a fault to the modeled event magnitude and peak ground motion in order to establish a method to translate quake parameters into mass wasting estimates. This has been performed for terrestrial examples focused on determining landslide area and density over time in seismically active regions [6]. We expect to find systematic variations in fit parameter estimates for each body, reflecting different gravitational strengths, regolith cohesion properties, and other geomorphic settings local to each study region.

References: [1] Watters, T. R. et al. (2015) *Geology* 43/10, 851–854. [2] Nahm, A. L. and Velasco, A. A. (2013) LPSC 44th, Abstract #1422. [3] Cowie, P. A. and Scholz, C. H. (1992) *J. Struct. Geol.* 14, 1149–1156. [4] Schmerr, N. et al. (2013) LPSC 44th, Abstract #2438. [5] Sjogreen, B. and Petersson, N. A. (2012) *J. Sci. Comp.* 52, 17–48. [6] Meunier, P. et al. (2007) *GRL* 23, doi:10.1029/2007GL031337.